DESIGN OF THE RISP VACUUM SYSTEMS

D. Jeon†, K.B. Lim, J. Song, S. Yoon, J. Cho, H. Son, Instititute for Basic Science, Daejeon, Korea
T. Ha, H.S. Choi, Pohang Accelerator Laboratory, Pohang, Korea
B.C. Kim, K.P. Kim, Y.S. Kim, K.M. Kim, National Fusion Research Institute, Daejeon, Korea
S.R. In, Korea Atomic Energy Research Institute, Daejeon, Korea

Abstract

The vacuum requirement of the RISP heavy ion accelerator facility has been derived that meets the beam loss requirement and the vacuum system design is carried out using the 3D Molflow code verifying the vacuum requirement. We used realistic outgassing values of the materials of the vacuum chambers and beam pipes. We are designing detailed vacuum system specification and configuration including pumps, gate valves, and vacuum gauges along with the interlock system and differential pumping stations.

VACUUM REQUIREMENT

The vacuum requirement for the RISP [1] is listed in Table 1 and determined to minimize the beam loss resulting from the interaction of the beam with the residual gas through electron capture, electron loss, nuclear reaction and Coulomb scattering etc [2-5].

Table 1: RISP Vacuum Requirement

System	Vac. level [mbar]	Remarks
ECR-IS	$3x10^{-7}$	
LEBT	$5x10^{-9}$	
RFQ	$5x10^{-8}$	
MEBT	$3x10^{-7}$	
SCL	$5x10^{-9}$	warm section
	$1x10^{-9}$	CM beam line vacuum
CSS	$1x10^{-6}$	Li charge stripper
	$1x10^{-8}$	beam line vacuum
IF	$1x10^{-6}$	IF target
	$1x10^{-7}$	separator beam vacuum
ISOL	$5x10^{-8}$	target
	$1x10^{-8}$	beam line

VACUUM SYSTEM

Realistic values are used for outgassing rates in designing the RISP vacuum system. For Annealed OFE copper, the outgassing rate is assumed to reach $1x10^{-10}$ mbar·L/s·cm^2 after 100-hour vacuum pumping and RF conditioning. This is based on the measured values for APT/LEDA CCDTL, SNS DTL, CCL. In case of SUS304 the outgassing rate is assumed to reach $1x10^{-10}$ mbar·L/s·cm^2 after 4 hour pumping with degreasing and acid cleaning. The outgassing rate of niobium after chemical etching, high pressure rinsing and baking is considered zero.

Driver Linac Injector

The driver linac injector consists of a 28-GHz superconducting ECR ion source (ECR IS), the LEBT, the 500-keV/u RFQ and the MEBT. For the ECR IS, superconducting magnets and dual high power RF sources of 28 GHz and 18 GHz are used to improve its performance.

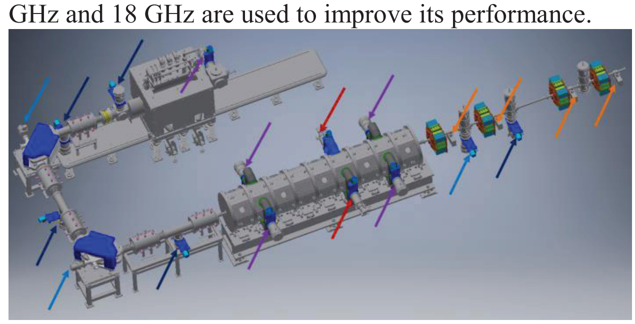

Figure 1: Integrated injector Molflow simulation model.

Table 2: Injector Vacuum System

Section	Pump	Speed	Number
LEBT Dipole	TMP	> 450 L/s	2
LEBT beam line	TMP	> 800 L/s	4
RFQ	Cryo	> 1700 L/s	2
	TMP	> 1100 L/s	4
MEBT	SIP	> 80 L/s	4
	TMP	> 450 L/s	1
	TMP	> 800 L/s	1

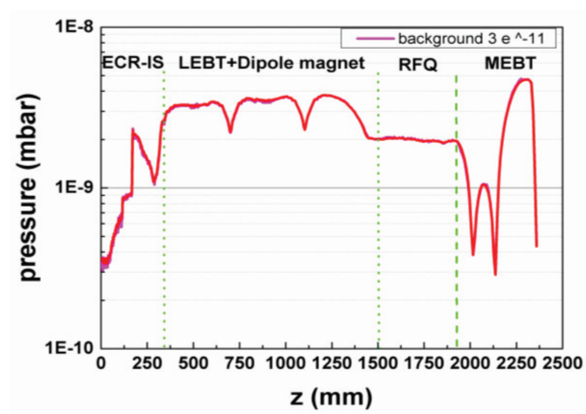

Figure 2: Plot of injector pressure profile.

Detailed vacuum structure is modelled and used as an input to the Molflow code, as shown in Fig. 1. Figure 2 shows the pressure profile along the injector. In the MEBT, there is a differential pumping station (DPS) be-

† jeond@ibs.re.kr

ISBN 978-3-95450-147-2

fore the superconducting linac to prevent the contamination of the cold linac along with the fast-closing shutter as the vacuum interlock. Table 2 lists the required pump types and the configuration of the injector vacuum system.

Superconducting Linac (SCL)

Because the superconducting linac is modular and periodic, analysis of one period (one cryomodule + warm section) is sufficient. Vacuum related structure of the superconducting linac is extracted and used as an input for the analysis. Figure 3 shows the vacuum related structure of the QWR section. Analysis indicates that 150-L/s pumping at the warm section is sufficient to achieve the vacuum level at the room temperature. The maximum pressure level is 8.3×10^{-8} mbar which is less than 5×10^{-5} mbar. At 4K operating temperature, the maximum pressure at the warm section meets the requirement of 5×10^{-9} mbar as shown in Fig. 4.

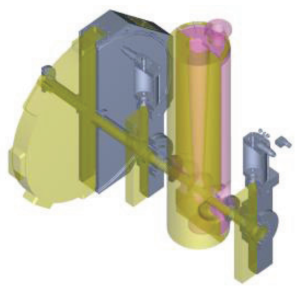

Figure 3: Simulation model of the QWR section.

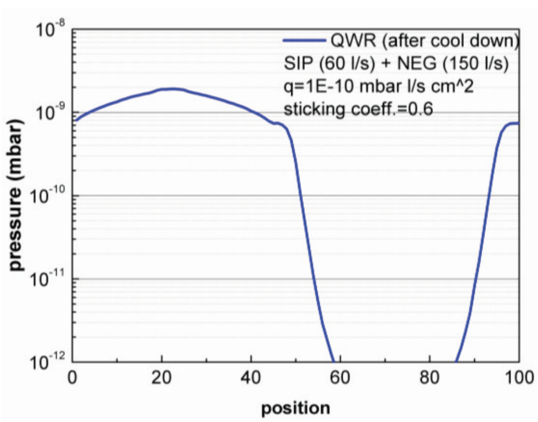

Figure 4: Plot of the QWR section pressure profile at 4K. 150-L/s pumping at the warm section is sufficient to meet the requirement.

Figure 5 shows the vacuum related structure of the HWR section. Analysis indicates that 200-L/s pumping at the warm section is sufficient to achieve the vacuum level at the room temperature. The maximum pressure level is 6.6×10^{-7}mbar meeting the requirement for cool-down. At 2K operating temperature of cavities, the maximum pressure at the warm section meets the requirement of 5×10^{-9} mbar as shown in Fig. 6.

Figure 7 shows the vacuum related structure of the SSR2 section where a cryomodule contains six SSR2 type cavities. Analysis indicates that 300-L/s pumping at the warm section is sufficient to achieve the vacuum level at the room temperature. At 2K operating temperature, the maximum pressure at the warm section meets the requirement of 5×10^{-9} mbar as shown in Fig. 8.

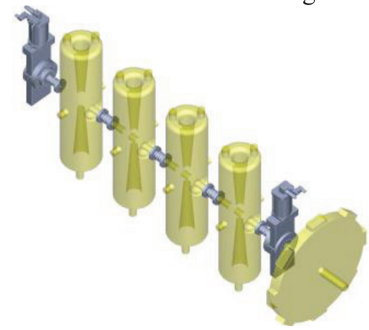

Figure 5: Simulation model of the HWR section.

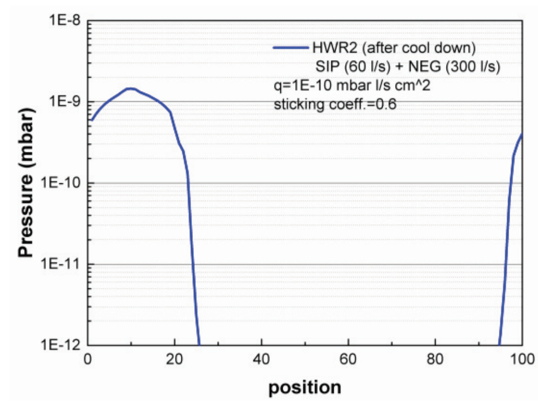

Figure 6: Plot of the HWR section pressure profile at 2K. 200-L/s pumping at the warm section is sufficient to meet the requirement.

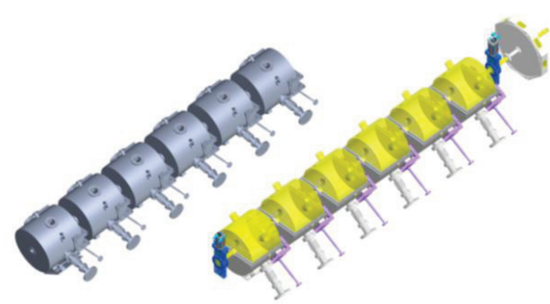

Figure 7: Simulation model of the SSR section.

Analysis finds the following for the superconducting linac vacuum system:

- Separate vacuum manifold in the cryomodule is not necessary and the pumping at the warm section is sufficient.
- Surface treatment of 6.3S and EP are required for the warm section vacuum surface treatment to reduce the outgassing.
- Beam pipe, BPM, and diagnostics box etc in the warm section should be installed and in-situ 200°C baking is required to reduce the outgassing.
- In order to increase the conduction, a design change into a racetrack type flange to increase the cross section is needed.

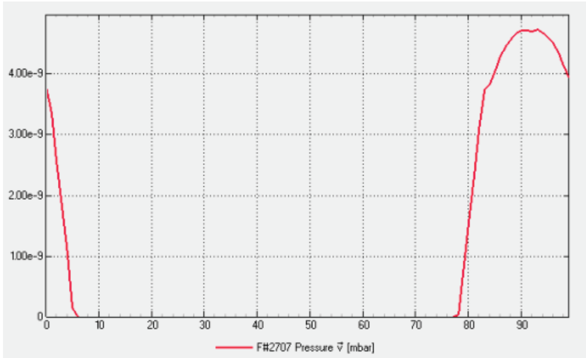

Figure 8: Plot of the SSR2 section pressure profile at 2K. 300-L/s pumping at the warm section is sufficient to meet the requirement.

Table 3: SCL Vacuum System

Section	Pump	Speed	Number
SCL11(QWR)	Ion/NEG	> 60/150 L/s	21
SCL12(HWR1)	Ion/NEG	> 60/300 L/s	13
SCL12(HWR2)	Ion/NEG	> 60/300 L/s	20
SCL21(SSR1)	Ion/NEG	> 300 L/s	23
SCL22(SSR2)	Ion/NEG	> 300 L/s	23

Charge Stripper Section (CSS)

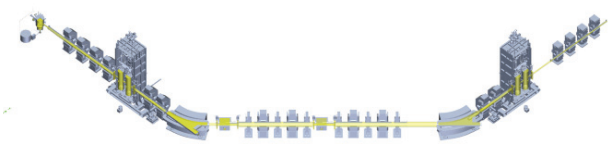

Figure 9: Simulation model of the CSS section. Yellow part is the vacuum pipe and RF cavities.

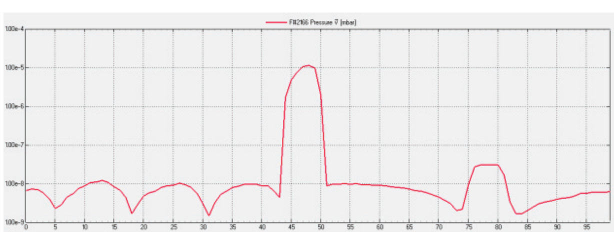

Figure 10: Plot of the CSS section pressure profile. The simulation confirms that the designed vacuum system meets the vacuum requirement.

Table 4: CSS Vacuum System

Section	Pump	Speed	Number
CSS	TMP	> 1000 L/s	2
	TMP	> 522 L/s	7
	TMP	> 250 L/s	2
	TMP	> 150 L/s	7

The Charge Stripper Section lies between the SCL1 and the SCL2 shown in Fig. 9 and consists of the liquid Li charge stripper, two HWR1-type cryomodules for beam bunching, collimators, and magnets. The main function is to strip off additional electrons from the accelerated heavy ion beams such as uranium. Vacuum profile is in Fig. 10. Table 4 lists the design vacuum system which meets the requirement.

Inflight Fragment (IF) System

The IF(Inflight Fragment) system follows the SCL2 which consists of carbon target, beam dump, pre-separators and main separator shown in Fig. 11. The function of the IF system is to produce rare isotope beams and to separate an RI beam of interest. Table 5 lists the vacuum pumps for the IF vacuum system.

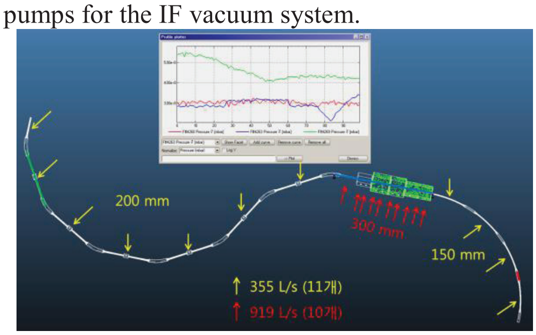

Figure 11: Plot of the CSS section pressure profile. The simulation confirms that the designed vacuum system meets the vacuum requirement.

Table 5: IF Vacuum System

Section	Pump	Speed	Number
IF hot cell	TMP	> 919 L/s	10
IF separators	TMP	> 355 L/s	7
HEBT	TMP	> 355 L/s	4

CONCLUSION

The vacuum requirement is derived to minimize the beam loss in each section of the accelerator. The design of the RISP vacuum system is carried out and 3D Molflow simulations confirm that the design meets the vacuum requirement.

ACKNOWLEDGEMENT

This work was supported by the Rare Isotope Science Project of the Institute for Basic Science funded by the MSIP and the NRF of Korea under Contract 2013M7A1A1075764.

REFERENCES

[1] D. Jeon *et al.*, *Design of the RAON accelerator systems*, J. Korean Phys. Soc. **65**, No. 7, 1010 (2014). DOI: 10.3938/jkps.65.1010

[2] A.S. Schachter *et al.*, Phys. Rev. A **27**, 3372 (1983).

[3] A.N. Perumal, Nucl. Instr. Meth. B **227**, 251 (2005).

[4] F.F. Rieke, Phys. Rev. **6**, 1507 (1972).

[5] G.H. Gillespie, Phys. Lett. **93A**, 327 (1983)

ISBN 978-3-95450-147-2